



Multiband Superconductivity of Heavy Electrons in a TlNi_2Se_2 Single Crystal

Hangdong Wang,^{1,2} Chiheng Dong,¹ Qianhui Mao,¹ Rajwali Khan,¹ Xi Zhou,¹
Chenxia Li,¹ Bin Chen,² Jinhu Yang,² Qiping Su,² and Minghu Fang^{1,*}

¹Department of Physics, Zhejiang University, Hangzhou 310027, China

²Department of Physics, Hangzhou Normal University, Hangzhou 310036, China

(Received 5 May 2013; revised manuscript received 16 October 2013; published 12 November 2013)

We have made the first observation of superconductivity in TlNi_2Se_2 at $T_C = 3.7$ K, and it appears to involve heavy electrons with an effective mass $m^* = (14\text{--}20)m_b$, as inferred from the normal-state electronic specific heat and the upper critical field, $H_{C2}(T)$. We found that the zero-field electronic specific-heat data, $C_{es}(T)$ ($0.5 \text{ K} \leq T < 3.7 \text{ K}$) in the superconducting state can be fitted with a two-gap BCS model, indicating that TlNi_2Se_2 seems to be a multiband superconductor, which is consistent with the band calculation for the isostructural KNi_2S_2 . It is also found that the electronic specific-heat coefficient in the mixed state $\gamma_N(H)$ exhibits a $H^{1/2}$ behavior, which is considered as a common feature of the d -wave superconductors. TlNi_2Se_2 , as a d -electron system with heavy electron superconductivity, may be a bridge between cuprate- or iron-based and conventional heavy-fermion superconductors.

DOI: 10.1103/PhysRevLett.111.207001

PACS numbers: 74.70.Xa, 71.27.+a, 74.25.Op, 74.70.Tx

The standard heavy-fermion compounds containing Ce, Yb, and U ions undergo a continuous transition from a high-temperature phase in which the f electrons behave as if they are localized, to a low-temperature heavy-fermion liquid phase in which the f electrons appear to be delocalized with enormous effective masses m^* [1–3]. The heavy-fermion liquid ground state is unstable to the formation of superconductivity and magnetically ordered states. The superconductivity in these materials appears to be anisotropic with an energy gap with point or line nodes, indicative of superconducting electron pairing with angular momentum greater than zero (i.e., d wave) [1–3]. It is widely believed that the pairing of the superconducting electrons is mediated by magnetic fluctuations.

An intriguing possibility is the existence of charge order, rather than the usual magnetic order, in proximity to the heavy-fermion state. The materials KNi_2Se_2 [4] and KNi_2S_2 [5], in which the Ni ion has a mixed valence $\text{Ni}^{1.5+}$, have recently been shown to exhibit several remarkable physical properties. At high temperatures they have high resistivity and a constant magnetic susceptibility. The structural analysis reveals that they have at least three distinct subpopulations of Ni-Ni bond lengths. Upon cooling below $T_{\text{coh}} \sim 20$ K, the resistivity rapidly decreases, and the system enters a coherent heavy-fermion state with effective electron mass $m^* \sim 10m_b$, eventually giving way to superconductivity below $T_c \sim 1$ K. It was suggested [4,6] that the formation of a heavy-fermion state at low temperatures is driven by the hybridization of localized charges with conduction electrons, the coherent state competes with a charge-fluctuating state, facilitated by the mixed valency of Ni ions in this system. It raises a question whether the superconductivity in this system is unconventional (i.e., d wave), as that in the standard heavy-fermion compounds, or conventional, as that in the

Ni-pnictide compounds, such as LaNiAsO ($T_C = 2.75$ K) [7], BaNi_2As_2 ($T_C = 0.7$ K) [8] or SrNi_2P_2 ($T_C = 1.4$ K) [9]. Because of their instability in air, a relatively lower T_C , and the Schottky anomaly corresponding to impurities in the specific heat for these new Ni-chalcogenide superconductors KNi_2Se_2 ($T_C = 0.8$ K) and KNi_2S_2 ($T_C = 0.46$ K) polycrystalline samples, there have been few reports on the nature of the superconductivity.

TlNi_2Se_2 crystallizes in a tetragonal ThCr_2Si_2 -type structure (space group $I4/mmm$), shown in Fig. 1(a), the same as that of KNi_2Se_2 , Fe-arsenide superconductors such as $(\text{Ba}, \text{K})\text{Fe}_2\text{As}_2$ [10], $\text{BaFe}_{2-x}\text{Co}_x\text{As}_2$ [11], Co-based

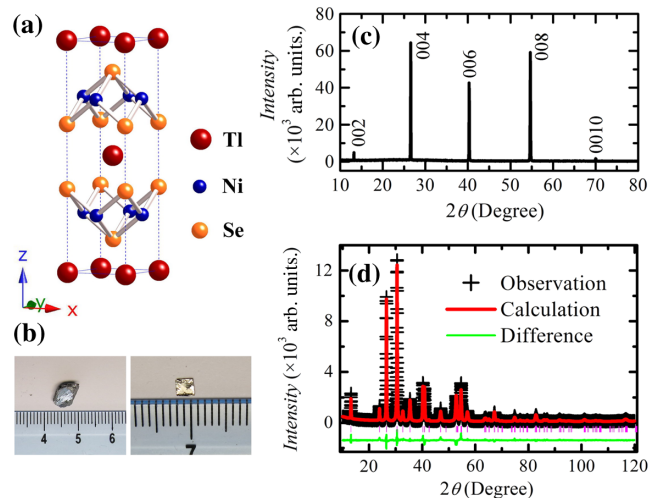


FIG. 1 (color online). (a) Crystal structure of stoichiometric TlNi_2Se_2 with the tetragonal ThCr_2Si_2 type. (b) Photos of TlNi_2Se_2 crystals (before being cleaved) and the TlNi_2Se_2 crystal. (c) Single-crystal XRD pattern of TlNi_2Se_2 and (d) XRD pattern of powder obtained by grinding TlNi_2Se_2 crystals. Its Rietveld refinement is shown by the solid lines.

superconductor LaCo_2B_2 [12], as well as the first heavy-fermion superconductor CeCu_2Si_2 [13]. It can be considered as one analog of Fe-chalcogenide superconductors recently discovered by us, i.e., TlFe_xSe_2 compounds with Fe vacancies [14,15]. The TlNi_2Se_2 compound is a Pauli paramagnetic metal, reported first by Newmark [16], who did not observe any superconducting transition above 2 K. For this Letter, we successfully grew a TlNi_2Se_2 single crystal and rechecked its structure and physical properties. Superconductivity was observed in TlNi_2Se_2 at $T_C = 3.7$ K and appears to involve heavy electrons with an effective mass $m^* = (14\text{--}20)m_b$. We found that the zero-field electronic specific-heat data, $C_{\text{es}}(T)$, ($0.5 \text{ K} \leq T < T_C$) in the superconducting state can be fit by a two-gap BCS model, indicating that TlNi_2Se_2 is a multiband superconductor. It is also found that the electronic specific-heat coefficient in the mixed state, $\gamma_N(H)$, exhibits a $H^{1/2}$ behavior, which was once considered as a common feature of the d -wave superconductors. Although we cannot conclude that the superconducting order parameter is s wave or d wave based on these results, TlNi_2Se_2 , as a d -electron system with heavy-electron superconductivity, seems to be a bridge between Fe-based and standard heavy-fermion superconductors.

Single crystals of TlNi_2Se_2 were grown using a self-flux method. A mixture with a ratio of $\text{Tl:Ni:Se} = 1:2:2$ was placed in an alumina crucible, sealed in an evacuated quartz tube, heated at 950°C for 12 h, and cooled to 700°C at a rate of 6°C/h , followed by furnace cooling. In each step to prepare the sample, we managed carefully due to the poison of the Tl metal. Single crystals with a typical dimension of $2 \times 2 \times 0.2 \text{ mm}^3$ [see Fig. 1(b)], were mechanically isolated from the flux. An energy dispersive x-ray spectrometer was used to determine the crystal composition, and stoichiometric TlNi_2Se_2 was confirmed, which is different with the analog of the Fe-chalcogenide compound, such as the TlFe_xSe_2 compound, in which Fe vacancies always exist [14]. The exact composition of TlNi_2Se_2 indicates that Ni ions should be a mixed valance of $\text{Ni}^{1.5+}$ due to Tl with a monovalence. The x-ray diffraction (XRD) pattern [see Fig. 1(d)] at room temperature of the TlNi_2Se_2 powder created by grinding pieces of crystals confirms its ThCr_2Si_2 -type structure, and its Rietveld refinement (weighted profile factor $R_{\text{WP}} = 9.53\%$, and the goodness-of-fit $\chi^2 = 2.671$) gives the lattice parameters of $a = 3.870(\pm 0.001) \text{ \AA}$ and $c = 13.435(\pm 0.001) \text{ \AA}$ and evidence of an absence of vacancies existing at each site. Electrical resistivity, both in-plane (ρ_{ab}) and out-of-plane (ρ_c), specific-heat C , and magnetic susceptibility χ measurements between 0.5 and 300 K were made using a Quantum Design Magnetic Property Measurement System or Physical Property Measurement System.

The physical properties of TlNi_2Se_2 are summarized in Fig. 2. Both ρ_{ab} and ρ_c vs T curves, shown in Fig. 2(a) and

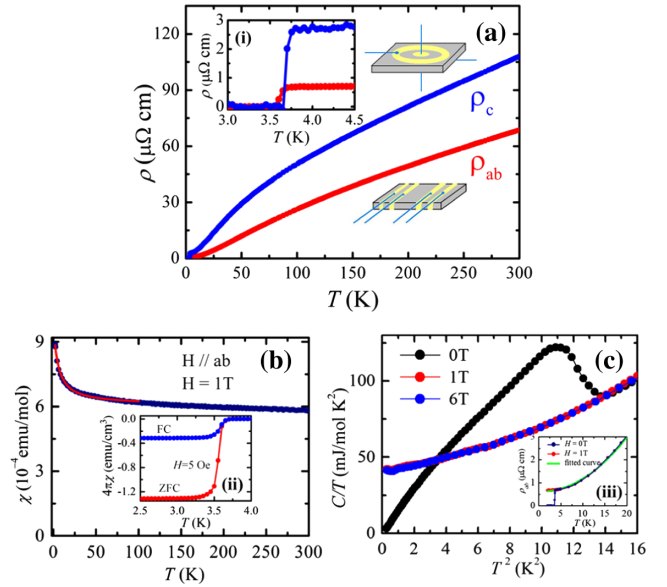


FIG. 2 (color online). (a) Temperature dependence of both in- and out-of-plane resistivity, $\rho_{ab}(T)$ and $\rho_c(T)$ for the TlNi_2Se_2 single crystal. (b) Temperature dependence of the normal-state magnetic susceptibility $\chi(T)$, measured at the 1 T field parallel to the ab plane. (c) Specific heat divided by temperature, C/T vs T^2 , measured under 0, 1, and 6 T fields. Inset: (i) $\rho_{ab}(T)$ and $\rho_c(T)$ near the superconducting transition, (ii) $\chi(T)$ near the superconducting transition, measured at 5 Oe field parallel to the ab plane (for minimizing the demagnetization factor) with both the zero-field cooling (ZFC) and field cooling (FC) processes, (iii) $\rho_{ab}(T)$ below 20 K measured under 0 and 1 T, the solid line indicates the fitting line using Fermi-liquid behavior.

inset (i), display a metallic behavior in the normal state before dropping abruptly to zero when superconductivity occurs at $T_C = 3.7$ K, which is also confirmed by a large diamagnetic signal [see the inset (ii) of Fig. 2] and a specific-heat jump at T_C as shown in Fig. 2(c). First, we discuss the resistivity in the normal state. ρ_{ab} and ρ_c at 300 K is 68.69 and 108.10 $\mu\Omega \text{ cm}$, respectively, and $\rho_c/\rho_{ab} = 1.57$, indicating that the anisotropy in the TlNi_2Se_2 is rather small, although the compound has a layered structure. In order to ascertain the $\rho_{ab}(T)$ behavior at low temperatures, we measured $\rho_{ab}(T)$ at various magnetic fields above the upper critical field [$\mu_0 H_{c2}(0) = 0.802 \text{ T}$, discussed below]. It was found that no change in $\rho_{ab}(T)$ measured at $\mu_0 H \geq 1$ up to 6 T occurs, indicating no magneto-resistance response in the normal state. In addition, we found that $\rho_{ab}(T)$ data below 25 K in the normal state can be very well described by a Fermi-liquid behavior, i.e., $\rho_{ab}(T) = \rho_0 + AT^2$, where $\rho_0 = 0.615 \mu\Omega \text{ cm}$ and $A = 4.94 \times 10^{-3} \mu\Omega \text{ cm/K}^2$ were obtained by fitting $\rho_{ab}(T)$ data measured at 1 T [see the green line in the inset (iii) of Fig. 2]. The residual resistivity ratio [$\text{RRR} = \rho_{ab}(300 \text{ K})/\rho_{ab}(2 \text{ K}) \sim 103$, where $\rho_{ab}(2 \text{ K})$ is obtained from $\rho_{ab}(T)$ data measured at 1 T] and superconducting transition width $\Delta T_C = 0.05 \text{ K}$ reflect the high quality of the single crystals. It is worth

noting that no discontinuous change in either $\rho_{ab}(T)$ or $\rho_c(T)$ was observed, which occurs in both isostructural BaNi_2As_2 [17] and SrNi_2P_2 [9] compounds, corresponding to the structural transition from a tetragonal at higher temperatures to a triclinic at lower temperatures. The powder XRD results (not shown in the Letter) at low temperatures also provide evidence that no structural transition occurs in the TlNi_2Se_2 compound below 300 K.

Now, we discuss the normal-state specific-heat $C_N(T)$ measured at a magnetic field $\mu_0 H = 6$ T, as shown in Fig. 2(c). The $C_N(T)/T$ vs T^2 plot below 4 K shows a pronounced nonlinear behavior, similar to that observed in KNi_2S_2 [4]. We therefore fitted $C_N(T)$ with $C_N(T) = \gamma_N T + \beta T^3 + \delta T^5$, which yields $\gamma_N = 40$ mJ/mol K², $\beta = 1.65$ mJ/mol K⁴, and $\delta = 0.135$ mJ/mol K⁶. The Debye temperature Θ_D was estimated to be of 175 K. The normal-state electronic specific-heat coefficient γ_N value corresponds to a mass enhancement $m^*/m_b = 14$ (assuming 1.5 carriers/Ni and a spherical Fermi surface). This value is comparable to that of the isostructural KNi_2Se_2 superconductor (44 mJ/mol K²) [4] and p -wave superconductor Sr_2RuO_4 (40 mJ/mol K²) [18], but is larger than that in Ni-arsenide superconductors, such as $\text{LaO}_{1-x}\text{F}_x\text{NiAs}$ (7.3 mJ/mol K²) [7] and BaNi_2As_2 (12.3 mJ/mol K²) [17], while it is much smaller than that in the standard heavy-fermion superconductors, such as CeCu_2Si_2 (1100 mJ/mol K²) [13], indicating that the electronic correlation in TlNi_2Se_2 is stronger than that in Ni-arsenide superconductors, but much weaker than that in the standard heavy-fermion superconductors. The Kadowaki-Woods ratio, A/γ^2 , relates the electronic specific heat to the temperature coefficient in the $\rho_{ab}(T) = \rho_0 + AT^2$, and is typically $\sim 10^{-5} \mu\Omega \text{ cm} (\text{mol K}^2 \text{ mJ})^2$ for the standard heavy-fermion systems [19,20]. For TlNi_2Se_2 , we calculate $A/\gamma^2 \sim 0.308 \times 10^{-5} \mu\Omega \text{ cm} (\text{mol K}^2 \text{ mJ})^2$, which identifies the metallic properties of TlNi_2Se_2 with heavy-fermion behavior.

As discussed by Takayama *et al.* [21] for a new strong-coupling superconductor SrPr_3P , we analyze the normal-state magnetic susceptibility $\chi(T)$, shown in Fig. 2(b), measured at a magnetic field of 1 T for the TlNi_2Se_2 crystal. $\chi = \chi_0 + \chi_{\text{CW}}$, where $\chi_0 = \chi_P + \chi_{\text{VV}} + \chi_{\text{core}}$ is a temperature independent contribution that includes a Pauli paramagnetism (χ_P), van Vleck paramagnetism (χ_{VV}), and core diamagnetism (χ_{core}), and χ_{CW} is a Curie-Weiss-like contribution (< 100 K), likely from magnetic impurities [as shown as the fitting red line in Fig. 2(b) corresponding to < 0.97 mol% of an $S = 1$ impurity, e.g., Ni^{2+}]. By subtracting the Curie-Weiss-like contribution, we estimate the temperature independent magnetic susceptibility as $\chi_0 = 6.064 \times 10^{-4}$ emu/mol. The core diamagnetic is estimated to be $\sim -0.76 \times 10^{-4}$ emu/mol by using those reported for Tl^{1+} , Ni^{2+} , and Se^{4+} . Then, the Pauli paramagnetic susceptibility is estimated to be $\chi_P = 6.824 \times 10^{-4}$ emu/mol by neglecting χ_{VV} , which, combined with $\gamma_N = 40$ mJ/mol K²,

yields the Wilson ratio $R_W = \pi^2 k_B^2 \chi_P / 3 \mu_B^2 \gamma_N = 1.24$, typical of many heavy-fermion compounds, being comparable to the value of KNi_2Se_2 ($R_W = 1.71$) [4], larger than the value ($R_W = 1.0$) of the free electron. We note that the Wilson ratio R_W value may be smaller than the value estimated above without subtracting the van Vleck paramagnetism contribution.

Then, we discuss the electronic specific heat in the superconducting state of TlNi_2Se_2 crystals. Fortunately, no Schottky anomaly in $C(T)$ measurements, at least at $T \geq 0.5$ K and $\mu_0 H \leq 6$ T, was observed for TlNi_2Se_2 single crystal, shown in Fig. 2(c), which allows us to make the analysis on the specific-heat data in the superconducting state. Based on the normal-state specific-heat C_N and γ_N obtained above, the zero-field electronic specific-heat C_{es} in the superconducting state was estimated as shown in Fig. 3(a), i.e., $C_{\text{es}} = C(0T) - C_{\text{latt}}$, where C_{latt} is the phonon contribution by fitting the C data measured at 6 T. At first, we try to fit the C_{es} data at low temperatures using a one-gap BCS model $C_{\text{es}} = C_0 \exp(-\Delta/k_B T)$, where k_B is the Boltzmann constant. It was found that low-temperature ($T < 1/4T_C$) specific-heat data can be described [see the inset of Fig. 3(a)], and the gap $\Delta = 3.03$ K by fitting, similar to that observed in the other Ni-arsenate compounds [8,9]. It should be pointed out that we cannot conclude the superconducting order parameter has s -wave symmetry, because the lowest temperature (0.5 K) for our measurements is not so low, compared with $T_C = 3.7$ K. The thermal conductivity, or the angle-dependent specific-heat measurements at lower temperatures in the future may provide more information about this. At the same time, we found that the standard BCS model cannot well describe all the C_{es} data, while the two-gap BCS model presents the best fit to the C_{es}/T data [see Fig. 3(a)]. According to the phenomenological two-gap model, the heat capacity is taken as the sum of contributions from the two bands, each one following the BCS-type temperature dependence [22]. In Fig. 3(a), we plot the contributions from the two superconducting gaps, $\Delta_1 = 0.84 k_B T_C$ and $\Delta_2 = 2.01 k_B T_C$, as well as their sum (black line). The weight contributed from the first gap Δ_1 is about 0.25. Most recently, Lu *et al.* [23] calculated the electronic band structure and the correlation effect by means of the density functional theory (DFT) plus the Gutzwiller variational method for the isostructural KNi_2S_2 compound. Their result indicates that KNi_2S_2 is a kind of multi-orbital system with five Ni $3d$ orbitals near the Fermi level and the correlation effects of $3d$ local electrons lead to the mass enhancement. We believe that the two-gap behavior in $C_{\text{es}}(T)$ and the mass enhancement in TlNi_2Se_2 may also result from a complicated Fermi surface and the existence of the correlation effects. Of course, the multiband superconductivity in TlNi_2Se_2 remains to be confirmed by further angle-resolved photoemission spectroscopy (ARPES) and other experiments.

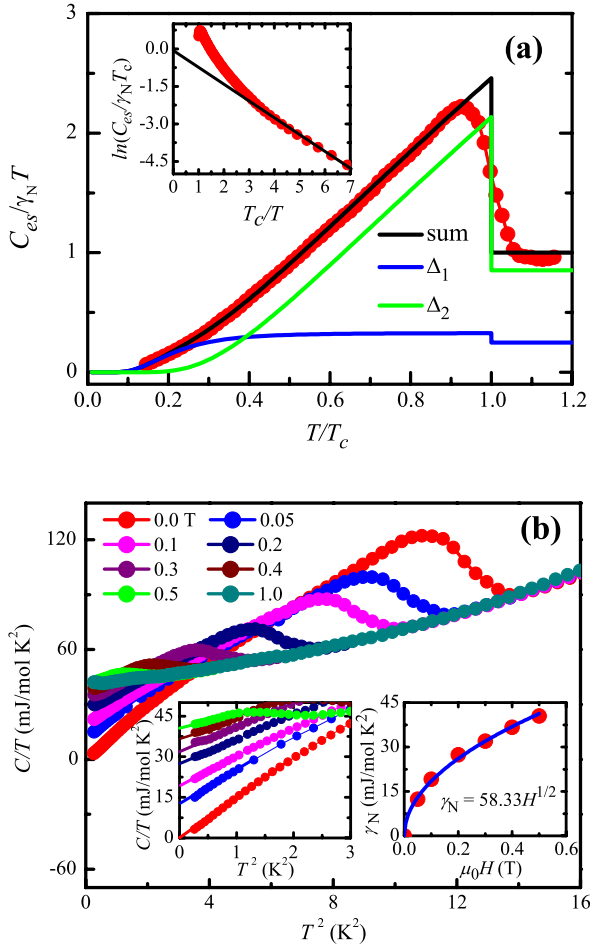


FIG. 3 (color online). (a) Reduced temperature T/T_C dependence of electronic specific heat divided by temperature C_{es}/T in the superconducting state at zero field, where $C_{es} = C - C_{latt}$. Three solid lines show the individual and total contributions of the two gaps to C_{es}/T , respectively. Inset: Reduced reciprocal temperature T_C/T vs reduced electronic specific-heat $C_{es}/\gamma_N T_C$. (b) Low-temperature specific heat divided by temperature C/T vs T^2 , measured at various fields near superconducting transition. Left inset: C/T vs T^2 blow 1.7 K. Right inset: Magnetic field $\mu_0 H$ dependence of electronic specific-heat coefficient γ_N in the mixed state.

In order to get more information about its superconducting gap, we also measured the low-temperature specific heat at various magnetic fields, $\mu_0 H < 1.0$ T as shown in Fig. 3(b) and the left inset in Fig. 3(b). At $\mu_0 H = 0$ T, zero linear electronic contribution of C_{es} indicates that almost 100% of the electrons enter the superconducting state, different from that (50%) observed in the polycrystalline KNi_2Se_2 [4] and KNi_2S_2 [5] samples. By increasing the magnetic field, the magnitude of the specific-heat jump at T_C decreases, and the linear electronic specific-heat coefficient, $\gamma_N(H)$, obtained by a linear extrapolation of C_{es}/T vs T^2 to $T = 0$ K, increases. In the mixed state, i.e., $H_{C1} < H < H_{C2}$ [where H_{C1} is the lower critical field, $H_{C1}(0) \sim 170$ Oe for TlNi_2Se_2 , determined by the magnetic

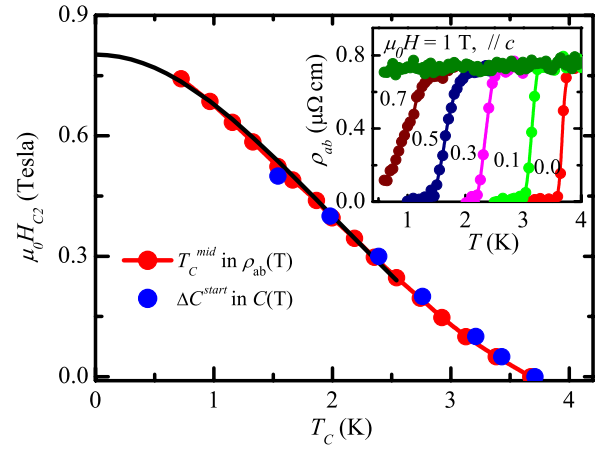


FIG. 4 (color online). Upper critical field H_{C2} vs T of TlNi_2Se_2 crystals. The superconducting transition temperature was determined by both the middle temperature of transition in $\rho_{ab}(T)$ and the starting temperature of the jump in $C(T)$ measured at different magnetic fields, $H \parallel c$ axis. Inset: in-plane resistivity, $\rho_{ab}(T)$ in magnetic fields up to 1.0 T applied parallel to the c axis.

hysteresis, $M(H)$, measurements at different $T < T_C$, not shown in the Letter], the electronic contribution to specific heat is usually attributed to the normal-state electrons in the core of vortex. For the s -wave superconductors, the cores contribute to C_{es} as a normal metal, and it should be in proportion to the numbers of the cores, i.e., $\gamma_N(H) = \gamma_0 H/H_{C2}$. However, we found that $\gamma_N(H) = 58.33 H^{1/2}$, as shown in the right inset of Fig. 3(b), obtained by fitting the $\gamma_N(H)$ data, which was generally observed in d -wave cuprate superconductors [24,25] and some heavy-fermion compounds, such as UPt_3 [26], due to the importance of the Doppler shift to d -wave superconductivity. The $\gamma_N(H) \propto H^{1/2}$ behavior was once considered as a common feature of the d -wave superconductors. It implies that superconductivity in TlNi_2Se_2 may also be unconventional, similar to that in the standard heavy-fermion superconductors, although this behavior was also observed in other s -wave superconductors, such as NbSe_2 [27,28], V_3Si [29], and CeRu_2 [30].

Finally, we present the analysis of the upper critical field $H_{C2}(T)$, which gives evidence for superconductivity from the heavy-mass electronic state in TlNi_2Se_2 , similar to that described for the standard heavy-fermion superconductors, such as for UBe_{13} [31]. Figure 4 presents the $H_{C2}(T)$ curve for TlNi_2Se_2 derived from $\rho_{ab}(T)$ (inset of Fig. 3) and $C_{es}(T)$ measurements as a magnetic field applied parallel to the c axis. It can be seen from Fig. 4 that the $H_{C2}(T)$ curves determined from both measurements are almost the same, especially for the temperature range near T_C . Using the middle superconducting transition temperature in $\rho_{ab}(T)$, the zero-temperature upper critical field $H_{C2}(0)$ can be estimated with a formula $H_{C2}(T) = H_{C2}(0) \times (1 - t^2)/(1 + t^2)$ [7,32], where t is the reduced temperature $t = T/T_C$, yielding the value of $\mu_0 H_{C2}(0) = 0.802$ T by fitting (see the main panel of Fig. 4). The

superconducting coherence length ξ_0 can be estimated from the relation $\xi_0 = (\Phi_0/2\pi H_{c2})^{1/2}$, yielding $\xi_0 = 20.3$ nm. A value for the Fermi velocity $v_F = 5.484 \times 10^4$ m/s is then obtained from $\xi_0 = 0.18\hbar v_F/k_B T_C$ [32] from which m^* and γ_N can be estimated below. Using a spherical Fermi surface approximation, the Fermi wave vector is given by $k_F = (3\pi^2 Z/\Omega)^{1/3}$, where Z is the number of electrons per unit cell and Ω is the unit cell volume. Assuming that Ni contributes 1.5 electrons ($Z = 6$), we obtain $k_F = 9.6 \times 10^9$ m $^{-1}$. The expression $m^* = \hbar k_F/v_F$ yields $m^* \sim 20m_b$. From the relation $\gamma_N = \pi^2 N k_B^2 m^*/\hbar^2 k_F^2$, $\gamma_N \sim 61$ mJ/mol K 2 . The values of m^* and γ_N are comparable to the values estimated from the normal-state specific heat. In addition, we also note that the $H_{c2}(T)$ curve has a positive curvature close to T_C , which is a typical feature observed for $R\text{Ni}_2\text{B}_2\text{C}$ ($R = \text{Y, Lu}$) [33] and MgB_2 [34,35] superconductors and can be explained by taking into account the dispersion of the Fermi velocity using an effective two-band model for superconductors in the clean limit. This result is consistent with the fact that $C_{es}(T)$ data can be fitted with a two-gap BCS model discussed above.

In summary, TlNi_2Se_2 exhibits superconductivity at $T_C = 3.7$ K, which appears to involve heavy electrons with an effective mass $m^* = (14\text{--}20)m_b$, as inferred from the electronic specific-heat coefficient γ_N and the upper critical field, $H_{c2}(0)$. We found that the zero-field electronic specific-heat data, $C_{es}(T)$, (0.5 K $\leq T < 3.7$ K) can be fitted with a two-gap BCS model, combined with the recent calculation of the band structure for the isostructural KNi_2S_2 [23], indicating that TlNi_2Se_2 may be a multiband superconductor. It is also found that the electronic specific-heat coefficient in the mixed state, $\gamma_N(H)$, exhibits a $H^{1/2}$ behavior, which was once considered as a common feature of the d -wave superconductors. This result indicates that superconductivity in TlNi_2Se_2 may be unconventional. Of course, it is necessary to confirm the unconventional superconductivity in TlNi_2Se_2 by means of other experiments, such as the thermal conductivity, angle-dependent specific heat, ARPES and nuclear magnetic resonance (NMR) measurements at lower temperatures in the future. Anyway, TlNi_2Se_2 , as a d -electron system with heavy-electron superconductivity, seems to bridge the gap between cuprate- or iron-based and conventional heavy-fermion superconductors.

This work is supported by the National Basic Research Program of China (973 Program) under Grants No. 2011CBA00103, No. 2012CB821404, and No. 2009CB929104, the National Science Foundation of China (Grants No. 11374261, No. 10934005, and No. 11204059) and Zhejiang Provincial Natural Science Foundation of China (Grant No. LQ12A04007), and the Fundamental Research Funds for the Central Universities of China (Grant No. 2013FZA3003). We thank Professor K. Yoshimura, Professor F. C. Zhang, and Dr. X. F. Xu for helpful discussions.

*mhfang@zju.edu.cn

- [1] Z. Fisk, H. R. Ott, T. M. Rice, and J. L. Smith, *Nature (London)* **320**, 124 (1986).
- [2] R. Heffner and M. Norman, *Comments Condens. Matter Phys.* **17**, 361 (1996).
- [3] G. R. Stewart, *Rev. Mod. Phys.* **56**, 755 (1984).
- [4] J. R. Neilson, Anna Llobet, A. V. Stier, L. Wu, J. Wen, J. Tao, Y. Zhu, Z. B. Tesanovic, N. P. Armitage, and T. M. McQueen, *Phys. Rev. B* **86**, 054512 (2012).
- [5] J. R. Neilson, T. M. McQueen, A. Llobet, J. J. Wen, and M. R. Suchomel, *Phys. Rev. B* **87**, 045124 (2013).
- [6] J. M. Murray and Z. Tesanovic, *Phys. Rev. B* **87**, 081103(R) (2013).
- [7] Z. Li *et al.*, *Phys. Rev. B* **78**, 060504(R) (2008).
- [8] F. Ronning, N. Kurita, E. D. Bauer, B. L. Scott, T. Park, T. Klimczuk, R. Movshovich, and J. D. Thompson, *J. Phys. Condens. Matter* **20**, 342203 (2008).
- [9] F. Ronning, E. Bauer, T. Park, S.-H. Baek, H. Sakai, and J. Thompson, *Phys. Rev. B* **79**, 134507 (2009).
- [10] M. Rotter, M. Tegel, and D. Johrendt, *Phys. Rev. Lett.* **101**, 107006 (2008).
- [11] A. S. Sefat, R. Jin, M. A. McGuire, B. C. Sales, D. J. Singh, and D. Mandrus, *Phys. Rev. Lett.* **101**, 117004 (2008).
- [12] H. Mizoguchi, T. Kuroda, T. Kamiya, and H. Hosono, *Phys. Rev. Lett.* **106**, 237001 (2011).
- [13] F. Steglich, J. Aarts, C. Bredl, W. Lieke, D. Meschede, W. Franz, and H. Schäfer, *Phys. Rev. Lett.* **43**, 1892 (1979).
- [14] M.-H. Fang, H.-D. Wang, C.-H. Dong, Z.-J. Li, C.-M. Feng, J. Chen, and H. Q. Yuan, *Europhys. Lett.* **94**, 27009 (2011).
- [15] H. D. Wang, C.-H. Dong, Z.-J. Li, Q.-H. Mao, S.-S. Zhu, C.-M. Feng, H. Q. Yuan, and M.-H. Fang, *Europhys. Lett.* **93**, 47004 (2011).
- [16] A. R. Newmark, G. Huan, M. Greenblatt, and M. Croft, *Solid State Commun.* **71**, 1025 (1989).
- [17] N. Kurita, F. Ronning, Y. Tokiwa, E. Bauer, A. Subedi, D. Singh, J. Thompson, and R. Movshovich, *Phys. Rev. Lett.* **102**, 147004 (2009).
- [18] S. Nishizaki, Y. Maeno, S. Farnar, S.-i. Ikeda, and T. Fujita, *J. Phys. Soc. Jpn.* **67**, 560 (1998).
- [19] K. Kadowaki and S. B. Woods, *Solid State Commun.* **58**, 507 (1986).
- [20] A. C. Jacko, J. O. Fjærestad, and B. J. Powell, *Nat. Phys.* **5**, 422 (2009).
- [21] T. Takayama, K. Kuwano, D. Hirai, Y. Katsura, A. Yamamoto, and H. Takagi, *Phys. Rev. Lett.* **108**, 237001 (2012).
- [22] F. Bouquet, Y. Wang, R. A. Fisher, D. G. Hinks, J. D. Jorgensen, A. Junod, and N. E. Phillips, *Europhys. Lett.* **56**, 856 (2001).
- [23] F. Lu, W. H. Wang, X. J. Xie, and F. C. Zhang, *Phys. Rev. B* **87**, 115131 (2013).
- [24] D. A. Wright, J. Emerson, B. Woodfield, J. Gordon, R. Fisher, and N. Phillips, *Phys. Rev. Lett.* **82**, 1550 (1999).
- [25] H. D. Yang and J. Y. Lin, *J. Phys. Chem. Solids* **62**, 1861 (2001).
- [26] H. P. van der Meulen, Z. Tarnawski, A. de Visser, J. Franse, J. Perenboom, D. Althof, and H. van Kempen, *Phys. Rev. B* **41**, 9352 (1990).

- [27] D. Sanchez, A. Junod, J. Muller, H. Berger, and F. Lévy, *Physica (Amsterdam)* **204B**, 167 (1995).
- [28] J.E. Sonier, M.F. Hundley, J.D. Thompson, and J.W. Brill, *Phys. Rev. Lett.* **82**, 4914 (1999).
- [29] A.P. Ramirez, *Phys. Lett. A* **211**, 59 (1996).
- [30] M. Hedo, Y. Inada, E. Yamamoto, Y. Haga, Y. Onuki, Y. Aoki, T.D. Matsuda, H. Sato, and S. Takahashi, *J. Phys. Soc. Jpn.* **67**, 272 (1998).
- [31] M.B. Maple, J. Chen, S. Lambert, Z. Fisk, J. Smith, H. Ott, J. Brooks, and M. Naughton, *Phys. Rev. Lett.* **54**, 477 (1985).
- [32] See, for example, M. Tinkham, *Introduction to Superconductivity* (McGraw-Hill, New York, 1975).
- [33] S.V. Shulga, S.-L. Drechsler, G. Fuchs, K.-H. Müller, K. Winzer, M. Heinecke, and K. Krug, *Phys. Rev. Lett.* **80**, 1730 (1998).
- [34] K.H. Müller, G. Fuchs, A. Handstein, K. Nenkov, V.N. Narozhnyi, and D. Eckert, *J. Alloys Compd.* **322**, L10 (2001).
- [35] S.L. Bud'ko, C. Petrovic, G. Lapertot, C.E. Cunningham, P.C. Canfield, M.H. Jung, and A.H. Lacerda, *Phys. Rev. B* **63**, 220503(R) (2001).